

# Growth and Characterization of $MgSO_4 \cdot 7H_2O$ Single Crystals Added With Urea/Thiourea

M.Vaitheeswari<sup>1</sup>, C.K.Mahadevan<sup>2</sup>Assistant Professor, Physics Research Centre, S.T. Hindu College, Nagercoil, Tamilnadu State, India<sup>1</sup>Professor, Center for Scientific and Applied Research, PSN College of Engineering and Technology, Tirunelveli,  
Tamilnadu State, India<sup>2</sup>

**ABSTRACT:**  $MgSO_4 \cdot 7H_2O$  is a hydrogen bonded crystal having wide application in various fields. Urea and thiourea (asorganic additives) were added (separately) into the  $MgSO_4 \cdot 7H_2O$  solution in different molar ratios and single crystals were grown by the free evaporation method at room temperature. The grown crystals were characterized structurally, chemically, thermally, optically, mechanically and electrically. The densities and lattice volumes observed indicate that the impurity molecules have entered into the host crystal matrix. All the eleven crystals grown are thermally stable upto about 70°C. Lower concentrated urea and higher concentrated thiourea additions are found to improve the optical transmittance. Results of microhardness measurements follow the normal indentation size effect. Results of electrical (AC and DC) measurements indicate that the grown crystals exhibit a normal dielectric behaviour and the electrical conduction is understood to be due to protonic movement. The present study indicates that urea/thiourea addition plays an important role in reducing the dielectric constant ( $\epsilon_r$ ) value significantly to make  $MgSO_4 \cdot 7H_2O$  crystal a low- $\epsilon_r$  value dielectric material, expected to be useful in the microelectronics industry.

**KEYWORDS:** Crystal growth, Electrical properties,  $MgSO_4 \cdot 7H_2O$  crystals, Mechanical properties, Optical properties, Single crystals.

## I. INTRODUCTION

$MgSO_4 \cdot 7H_2O$  (magnesium sulphate heptahydrate) crystals naturally formed are transparent to translucent. They are colourless to white with pale shades of pink and green. The molecular weight of  $MgSO_4 \cdot 7H_2O$  is 246.48. The chemical composition (as reported in Lapis Mineral Journal) is: Magnesium (Mg) - 9.86%, Hydrogen (H) - 5.73%, Sulphur (S) - 13.01%, and Oxygen (O) - 71.40%.

In dry air conditions,  $MgSO_4 \cdot 7H_2O$  may lose one molecule of water and convert to the very closely related material hexahydrate ( $MgSO_4 \cdot 6H_2O$ ). This changes the symmetry from orthorhombic in  $MgSO_4 \cdot 7H_2O$  to monoclinic in hexahydrate.  $MgSO_4 \cdot 7H_2O$  has numerous medical and pharmaceutical applications, for example, in the treatment of cardiac arrhythmia, acute, asthma, eclampsia and gallstones. It has been used in agriculture (fertilizer), cotton and silk manufacturing, ore processing and as an additive in explosives. It is a raw material for manufacturing various chemicals containing magnesium and also has applications in the field of dosimetric measurements and luminescence studies [1,2].  $MgSO_4 \cdot 7H_2O$  crystal is an example of hydrogen bonded systems and is isomorphous with  $NiSO_4 \cdot 7H_2O$  and  $ZnSO_4 \cdot 7H_2O$  crystals [3]. The crystal system is orthorhombic and there are 4 molecules per unit cell. The point group is 222 and the space group is  $P2_12_12_1$ . The lattice parameters obtained through X-ray powder diffraction measurements and reported in the JCPDS File (No:36-0419) are:  $a = 11.869(5)$ ,  $b = 11.984(5)$  and  $c = 6.847(1)$  Å. The measured and calculated density values reported here are 1.680 and 1.681  $g/cm^3$  respectively. The lattice parameters obtained from single crystal X-ray diffraction data [4] are:  $a = 11.868$ ,  $b = 11.996$  and  $c = 6.857$  Å.

Crystal growth of metal sulphate heptahydrate materials such as magnesium sulphate heptahydrate (hereafter represented as MSH) of high purity has become an important field of research for both academic interest and industrial applications [2,5,6]. During industrial crystallization, the size and shape of the crystal plays an important factor, since the undesirable habits such as plate-like or needle-like causes the problem of separating, washing or drying [7]. The

# International Journal of Innovative Research in Science, Engineering and Technology

(An ISO 3297: 2007 Certified Organization)

Vol. 4, Issue 7, July 2015

physical properties such as packing density, agglomeration and re – dissolution mainly depend on the shape of the crystal.

Pure MSH crystals have been grown at low temperature from aqueous solutions [8-13]. Presence of foreign particles in the growth media has long been recognized in changing the growth habits of crystals [14,15]. Jibbouri et al. [15] found that the impurities (KCl,  $K_2SO_4$ , NaCl and  $MgCl_2$ ) exert influence on the saturation and supersaturation limit. Ferdous and Podder [13] found that the optical quality of MSH crystal improves on doping with KCl. Also, their dielectric studies showed that KCl doped MSH possesses low dielectric constant and low dielectric loss which could be suitable for electro-optic applications. Mahadevan [12] has observed larger electrical conductivity values for the impurity (KCl and  $KNO_3$ ) added MSH single crystals. Mahadevan and his co-workers have reported on MSH forming mixed crystals with  $ZnSO_4 \cdot 7H_2O$  and  $NiSO_4 \cdot 7H_2O$  along with some other studies [16-18].

Previous authors have shown that impurity addition to MSH makes it a more interesting material [12-15]. The  $SO_4$  group in MSH may be considered similar to the  $PO_4$  group in potassium dihydrogen orthophosphate (KDP) and ammonium dihydrogen orthophosphate (ADP). A theoretical study [19] identified MSH as a promising thermochemical material (TCM) for long-term heat storage. The theoretical storage density of MSH is  $2.8 \text{ GJ/m}^3$  which offers a more compact way of storing energy for the same volume in comparison to water ( $0.25 \text{ GJ/m}^3$  in the temperature range  $25\text{-}85^\circ\text{C}$ ). Additionally, MSH is cheap, non-toxic and non-corrosive. For these reasons, MSH was studied by Van Essen and his co-workers [20] as a possible TCM for solar seasonal heat storage. The results of this study indicate that the application of MSH at atmospheric pressure is problematic for a heat storage system where heat is released above  $40^\circ\text{C}$  using a water vapour pressure of 1.3kPa. However, modification of the material as well as reducing the pressure may yield good results.

Microelectronics industry needs replacement of dielectric materials in multilevel interconnect structures with new low dielectric constant ( $\epsilon_r$ ) materials such as interlayer dielectric (ILD) which surrounds and insulates interconnect wiring. Lowering the  $\epsilon_r$  values of the ILD decreases the RC delay, lowers power consumption and reduces 'cross-talk' between nearby interconnects [21]. Silica has  $\epsilon_r \approx 4.0$ , in part as a result of the Si-O bonds. Several innovative developments have been made for the development of new low-  $\epsilon_r$  value materials to replace silica. However, there is still a need for new low -  $\epsilon_r$  value dielectric materials. As the utility is in the electronic circuits with water proof condition, water soluble material in the single crystal form would be very much interesting. Mahadevan and his co-workers [22,23] have reported the possibility of reducing the  $\epsilon_r$  value by adding simple organic molecules, namely, urea and L-arginine to KDP. Very recently, Kavitha and Mahadevan [24,25] have reported that glycine addition plays an important role in reducing the  $\epsilon_r$  value significantly to make Morenosite and Epsomite crystals low –  $\epsilon_r$  value dielectric materials.

Forming hybrid materials (by mixing or doping) with improved physical properties are very much needed for many emerging technologies. Aiming at discovering new useful materials, a research programme was planned and a series of investigations were undertaken in these laboratories on the growth and physical properties of some metal sulphate heptahydrate single crystals. As a part of the programme, in the present study, we have grown MSH single crystals by the free evaporation method and investigated the effect of two simple but interesting organic impurities (urea and thiourea) added (impurity added in the MSH solution used for the growth of crystals) with impurity concentration ranging from 2000 – 10000 ppm (i.e. 0.2-1.0 mole%) on their structural, thermal, optical, mechanical and electrical properties. A total of eleven crystals were grown and characterized. The results obtained are reported herein and discussed

## II. MATERIALS AND METHODS

### II.1. Growth of single crystals

Analytical reagent (AR) grade chemicals of  $MgSO_4 \cdot 7H_2O$ , urea and thiourea along with double distilled water were used for the growth of single crystals. Aqueous solution of  $MgSO_4 \cdot 7H_2O$  (pure or urea/thiourea added) was prepared at a supersaturated concentration and taken in a nucleation cell (100 ml beaker of corning glass) and allowed to equilibrate at the desired temperature. The crystals were grown in the unstirred condition and the temperature and volume were kept constant respectively at  $33^\circ\text{C}$  and 25ml for all the crystal growth experiments. Small crystals appeared in the

# International Journal of Innovative Research in Science, Engineering and Technology

(An ISO 3297: 2007 Certified Organization)

Vol. 4, Issue 7, July 2015

beginning due to slow evaporation of the solvent and grew larger in considerable finite time. Concentration programming was done to obtain good MSH single crystals by using various supersaturated concentrations between 2.8 and 3.5M. 3.15 M solution gave good MSH crystals and this concentration was considered for growing the impurity added MSH crystals also. Crystals were grown from pure ( $\text{MgSO}_4 \cdot 7\text{H}_2\text{O}$ ) and five (in each case) impurity (urea and thiourea) added (separately with impurity concentrations, viz. 0.2, 0.4, 0.6, 0.8 and 1.0 mole%) solutions. Best crystals formed were selected and used for the characterization experiments.

## II.2. Characterizations made

Na, K and Ca metal impurities were expected to be present in the crystal considering the Assay Information given by the supplier of AR grade  $\text{MgSO}_4 \cdot 7\text{H}_2\text{O}$ . So, in order to determine the concentrations of these impurities, atomic absorption spectroscopic (AAS) analysis was carried out for the pure  $\text{MgSO}_4 \cdot 7\text{H}_2\text{O}$  crystal using an atomic absorption analyser (Model: AA6300).

Densities of the grown crystals were determined by using the floatation method [26,27] within an accuracy of  $\pm 0.008 \text{g/cm}^3$ . Bromoform of density  $2.890 \text{g/cm}^3$  and carbon tetrachloride of density  $1.594 \text{g/cm}^3$  are respectively the rarer and denser liquids used.

As the impurities considered are organic compounds, no experiment was carried out to determine the impurity concentration in the crystals grown. However, an approximate method (using solubility data) was used to determine the impurity concentration in a way similar to that followed by Freeda and Mahadevan [28]. If X and Y are the initial concentrations ( $\text{g}/100 \text{cm}^3$ ) of A and B the final stoichiometry will be  $(X - A_x) : (Y - A_y)$  where  $A_x$  and  $A_y$  are the solubilities of components A and B respectively. If we simply use this relation, in the present study, we would get negative value for  $(Y - A_y)$ . So, in order to avoid this situation, we modified the above ratio as

$$(10000X - A_x) : (10000Y - A_y).$$

The values obtained are expected to be reasonable ones and any inaccuracy if present will be negligible and the percentage error will be within the tolerance limit. The molecular weight and solubility in water (at  $33^\circ\text{C}$ ) values used are: for MSH - 246.48 and  $115 \text{g}/100 \text{cm}^3$  water; for Urea - 60.1 and  $120 \text{g}/100 \text{cm}^3$  water; and for Thiourea - 76.1 and  $12 \text{g}/100 \text{cm}^3$  water. These values were estimated from the values available for other temperatures in the literature [9,29].

X-ray powder diffraction (PXRD) data were collected for all the eleven crystals grown by using an automated X-ray powder diffractometer (PANalytical) in the  $2\theta$  range  $10 - 70^\circ$  with  $\text{CuK}_\alpha$  radiation ( $\lambda = 1.54056 \text{\AA}$ ). The reflections observed were indexed using the data available in JCPDS File (No: 36 - 0419) following the procedures of Lipson and Steeple [30]. Lattice parameters were determined from the indexed data (high angle reflections) using the relation:

$$\sin^2 \theta_{hkl} = (\lambda^2/4) [(h^2/a^2) + (k^2/b^2) + (l^2/c^2)] \quad (1)$$

where  $\theta_{hkl}$  is the Bragg angle,  $\lambda$  is the wavelength of radiation used, h, k, l are the Miller indices and a, b, c are the unit cell edges.

Fourier transform infrared (FTIR) spectra were recorded by the KBr pellet method in the wavenumber range  $400 - 4000 \text{cm}^{-1}$  for all the eleven crystals grown by using a BRUKER IFS 66V FTIR spectrometer.

The UV-Vis-NIR transmittance spectra for all the eleven crystals grown (dissolved in water) were recorded by using a Lambda 35 spectrophotometer in the wavelength range 190-1100 nm.

The thermogravimetric analysis (TGA) was carried out by employing a Perkin Elmer thermogravimetric analyser (Model: PYRIS DIAMOND) in nitrogen atmosphere heated from  $50 - 830^\circ\text{C}$  with a heating rate of  $20^\circ\text{C}/\text{minute}$  for the pure and maximum concentrated impurity added MSH crystals.

Microhardness measurements were carried out at room temperature on all the eleven crystals grown (transparent and free from crack) by using a Vicker's microhardness indenter (Laitz-Weitzier hardness tester) with three loads, viz. 25, 50 and 100g for a dwell period of 10s. The indentation impressions on the well developed flat surface ((100) face) were observed to be square shaped and their size increased with the increase of applied load. For a particular load (P) several

# International Journal of Innovative Research in Science, Engineering and Technology

(An ISO 3297: 2007 Certified Organization)

Vol. 4, Issue 7, July 2015

well-defined impressions have been considered and the average of all the diagonals (d) has been considered. Vicker's hardness numbers ( $H_v$ ) were calculated using the relation:

$$H_v = 1.8544(P/d^2) \text{ kg/mm}^2 \quad (2)$$

Plots of  $\log P$  versus  $\log d$  were drawn and, from the slopes of these plots, the work hardening coefficients (Meyer index,  $n$ ) were also determined. The Meyer's law [31] used for this is expressed as:

$$P = K_1 d^n \quad (3) \quad \text{where } K_1 \text{ is the material constant.}$$

The DC and AC electrical measurements were carried out to an accuracy of  $\pm 2.5\%$  for all the eleven crystals grown in the present study along the  $c$ -direction (major growth direction) at various temperatures ranging from  $35-65^\circ\text{C}$ . Crystals with large surface defect free (i.e. without any pit or crack or scratch on the surface, tested with a travelling microscope) size ( $>3\text{mm}$ ) were selected and used. The extended portions of the crystals were removed completely and the opposite faces were polished and coated with good quality graphite to obtain a good conductive surface layer. The dimensions of the crystal were measured by using a travelling microscope (least count= $0.001\text{cm}$ ). Observations were made while cooling the sample crystal and the temperature was controlled to an accuracy of  $\pm 1^\circ\text{C}$ . The temperature range was fixed by considering the thermal stability of the grown crystals understood through the TGA measurement.

The DC resistance was measured by the conventional two-probe method using a million megohmmeter in a way similar to that followed by Mahadevan and his co-workers [32-34]. The DC electrical conductivity ( $\sigma_{dc}$ ) of the crystal was calculated using the relation:

$$\sigma_{dc} = d_{crys}/(RA_{crys}) \quad (4)$$

where  $R$  is the measured resistance,  $d_{crys}$  is the thickness of the sample crystal and  $A_{crys}$  is the area of the face of the crystal in contact with the electrode.

The capacitance ( $C_{crys}$ ) and dielectric loss factor ( $\tan\delta$ ) were measured by the parallel plate capacitor method using an LCR meter (Systronics make) with a fixed frequency of  $1 \text{ kHz}$  in a way similar to that followed by Mahadevan and his co-workers [35-37]. The air capacitance ( $C_{air}$ ) was measured only at the lower temperature considered as the temperature variation of air capacitance was found to be negligible. The dielectric constant ( $\epsilon_r$ ) of the crystal was calculated using Mahadevan's relation (as the crystal area was smaller than the plate area of the cell) [38,39]:

$$\epsilon_r = [A_{air}/A_{crys}][[C_{crys}-C_{air}][1-A_{crys}/A_{air}]/C_{air}] \quad (5) \quad \text{where } C_{crys} \text{ is the capacitance with crystal (including air) and } A_{air} \text{ is the area of the electrode.}$$

The AC electrical conductivity ( $\sigma_{ac}$ ) was calculated using the relation:

$$\sigma_{ac} = \epsilon_0 \epsilon_r \omega \tan\delta \quad (6)$$

where  $\epsilon_0$  is the permittivity of free space ( $8.85 \times 10^{-12} \text{ C}^2 \text{ N}^{-1} \text{ m}^{-2}$ ) and  $\omega$  is the angular frequency ( $\omega = 2\pi f$ ;  $f$  is the frequency =  $1 \text{ kHz}$ ) of the applied field..

## III. RESULTS AND DISCUSSION

### III.1. Crystals grown and densities

Crystals up to a maximum of  $2\text{cm}$  length were obtained. A photograph of the sample crystals grown is shown in Figure 1. All the eleven crystals grown are transparent without any colour. Morphologies of all the doped crystals grown are found to be similar to that of the pure MSH crystals. The crystals are found to be stable and non-hygroscopic in atmospheric air.

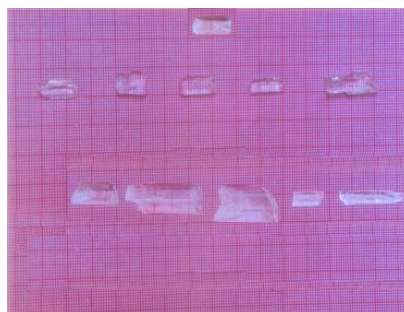


Figure 1: Photograph showing the sample crystals grown

# International Journal of Innovative Research in Science, Engineering and Technology

(An ISO 3297: 2007 Certified Organization)

Vol. 4, Issue 7, July 2015

[From left: Top row – Pure MSH;  
Middle row – Urea added(0.2,0.4,0.6,0.8,1.0 mole%);  
Bottom row – Thiourea added(0.2,0.4,0.6,0.8,1.0 mole%)]

The average densities observed are shown in Figure 2. The density value obtained for the pure MSH crystal in the present study ( $1.668 \text{ g/cm}^3$ ) compares well with that reported in the literature ( $1.677 \text{ g/cm}^3$  - in Handbook of Mineralogy, MinSoc Am). For the two impurities considered in the present study (urea and thiourea), the observed decrease of density of MSH crystal due to impurity addition indicates that the impurity molecules have entered into the MSH crystal matrix. It can be seen that the density decreases further with the increase in impurity concentration of the aqueous solution of MSH used for the growth of single crystals.

### III.2. Lattice parameters and chemical composition

Results of the AAS analysis indicate the presence of natural metallic impurities in trace amounts. The metallic impurities present in the pure MSH crystal are observed to be: Na – 468 ppm, K – 264 ppm and Ca – 172 ppm.

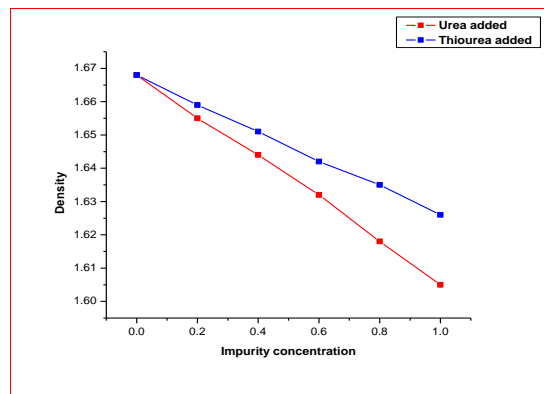


Figure 2: Variation of density ( $\text{g/cm}^3$ ) with impurity concentration (mole%)

The estimated impurity concentrations are shown in Figure 3. The estimated impurity concentration in the crystal shows that the impurity molecules are mainly occupying the interstitial positions. Moreover, the impurity concentrations considered in the present study are small. So, for impurity added MSH crystals, the impurity molecules may be considered to be added in the MSH crystal matrix in the same amount (ratio) as estimated.

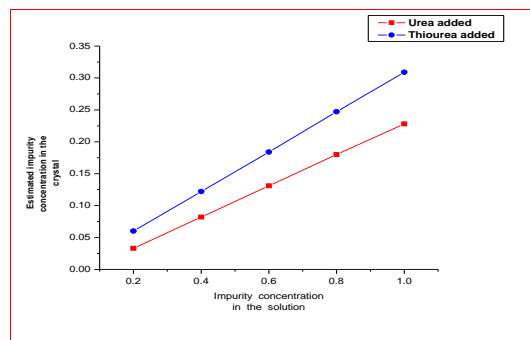


Figure 3: The estimated impurity concentration in the crystal (mole%) versus impurity concentration in the solution (mole%)

## International Journal of Innovative Research in Science, Engineering and Technology

(An ISO 3297: 2007 Certified Organization)

Vol. 4, Issue 7, July 2015

It is a known fact that urea and thiourea are simple organic substances and are expected to occupy the interstitial positions. If the probability of occupation of an interstice is  $\rho$ , then the probability of finding a vacant neighbour site is  $(1-\rho)$ . Even for very high concentrations, of the order of  $10^{20}/\text{cm}^3$ ,  $\rho$  does not exceed  $10^{-2}$  so that in real cases with concentration of interstitials of the order of  $10^{15} - 10^{20}/\text{cm}^3$ ,  $(1-\rho) \approx 1$  [40]. The impurity concentrations (taken in the solutions used for the growth of single crystals) considered in the present study are within this limit only. Also, the estimated impurity concentrations (in the crystals) are found to be very less when compared to that taken in the solution.

However, the density measurement shows a small decrease of density with the increase of impurity concentration. So, the impurity molecules can be assumed to replace the water molecules and ions ( $\text{Mg}^{2+}$  and  $\text{SO}_4^{2-}$ ) to a small level (atleast) in addition to occupying the interstitials in the MSH crystal matrix creating a random disturbance in the hydrogen-bonding system. This is expected to affect the molecular vibrations in the crystal in a random manner.

The PXRD patterns obtained in the present study are shown in Figures 4-5. Appearance of strong and sharp peaks confirm the crystalline nature of the sample crystals grown. The average lattice parameters obtained are given in Table 1. The lattice volume of pure MSH crystal obtained in the present study ( $984.73 \text{ \AA}^3$ ) compares well with that obtained from single crystal XRD data and reported ( $976.22 \text{ \AA}^3$ ) in the literature [4]. A small difference seen may be due to the difference in the techniques followed and instruments used. The observed PXRD patterns for the urea or thiourea added MSH crystals indicate that they are almost similar to that observed for the pure MSH crystal. This indicates that the incorporation of impurity molecules has not distorted the MSH lattice significantly.

For both the impurities considered in the present study (urea and thiourea), the observed decrease of lattice volume of MSH crystal caused by the impurity addition indicates that the impurity molecules have entered into the lattice of MSH crystals. The lattice volume decreases further with the increase of impurity concentration in the aqueous solution of MSH used for the growth of single crystals.

The FTIR spectra observed in the present study are shown in Figures 6-7. The observed characteristic vibrational frequencies are provided in Tables 2-3. The observed spectra for the urea or thiourea added MSH crystals indicate that they are almost similar to that observed for the pure MSH crystal. However, the small shift in the frequencies and intensities observed due to impurity addition endorses the results obtained in the PXRD analysis and density measurement. Thus, it can be understood that the impurity added MSH crystals are basically the MSH crystals without significant variation in the structural arrangement of constituent atoms but the impurity molecules have entered into the MSH crystal matrix either by replacement of  $\text{Mg}^{2+}$  and  $\text{SO}_4^{2-}$  ions and water molecules or by occupying the interstitial positions.

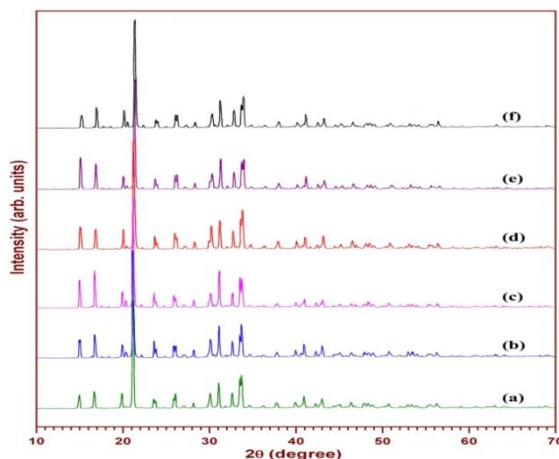


**Figure 4: The PXRD patterns for pure and urea doped MSH crystals [For (a) pure MSH, and for (b) 0.2, (c) 0.4, (d) 0.6, (e) 0.8, and (f) 1.0 mole% urea added MSH crystals]**

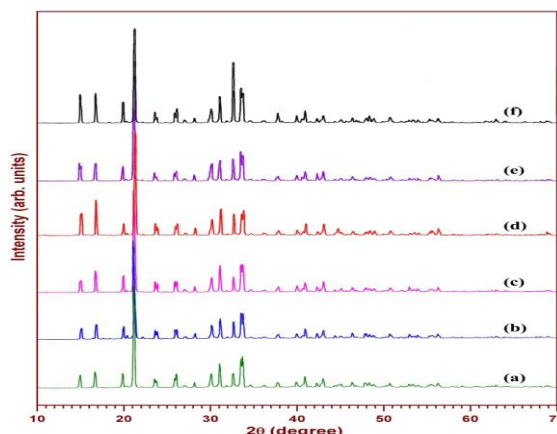


**Figure 5: The PXRD patterns for pure and thiourea doped MSH crystals [For (a) pure MSH, and for (b) 0.2, (c) 0.4, (d) 0.6, (e) 0.8, and (f) 1.0 mole% thiourea added MSH crystals]**

**Table 1: The lattice parameters observed for pure and impurity added MSH crystals**

System	Lattice parameters			
	a (Å)	b(Å)	c(Å)	V(Å <sup>3</sup> )
(Impurity in mole% in the solution)				
a) For pure MSH	12.080(83)	11.937(1)	6.829(34)	984.73
b) For urea added MSH				
0.2	11.860(2)	11.929(25)	6.945(31)	982.56
0.4	11.897(16)	12.178(1)	6.750(35)	977.95
0.6	11.780(14)	12.060(42)	6.847(40)	976.56
0.8	11.965(1)	12.029(31)	6.754(55)	972.08
1.0	11.781(10)	11.881(25)	6.890(18)	964.39
c) For thiourea addedMSH				
0.2	12.822(17)	11.984(1)	6.846(5)	969.91
0.4	11.604(26)	11.976(15)	6.863(1)	953.74
0.6	11.873(3)	11.591(22)	6.852(1)	942.97
0.8	11.823(17)	11.486(36)	6.834(12)	928.11
1.0	11.714(45)	11.804(89)	6.696(11)	925.87

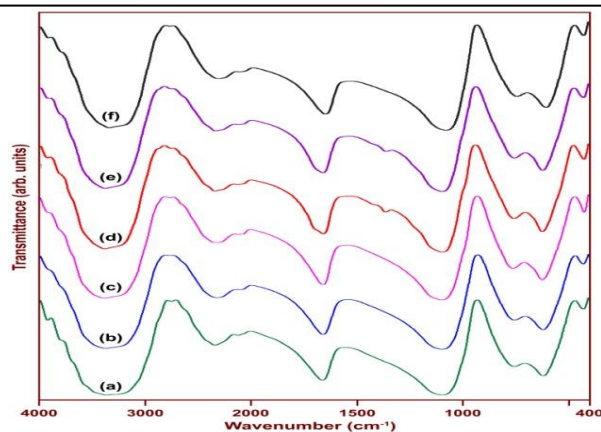


**Figure 6: The FTIR spectra of pure and urea added MSH crystals[For (a) pure MSH, and for (b) 0.2, (c) 0.4, (d) 0.6, (e) 0.8, and (f) 1.0 mole% urea added MSH crystals]**

## International Journal of Innovative Research in Science, Engineering and Technology

(An ISO 3297: 2007 Certified Organization)

Vol. 4, Issue 7, July 2015

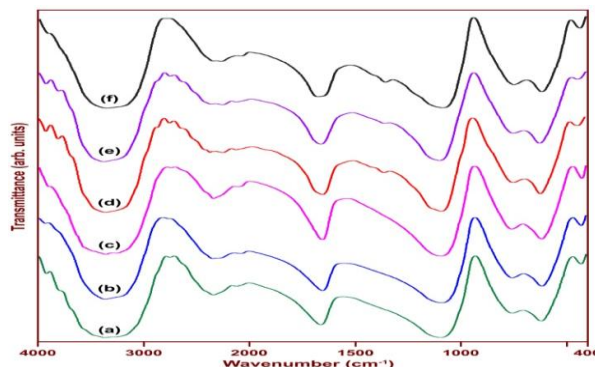


**Figure 7: The FTIR spectra of pure and thiourea added MSH crystals**  
[For (a) pure MSH, and for (b) 0.2, (c) 0.4, (d) 0.6, (e) 0.8, and (f) 1.0 mole% thiourea added MSH crystals]

**Table 2: The FTIR band assignments for pure and urea added MSH crystals**

Sl.No	Wave numbers (cm <sup>-1</sup> ) for						Band assignment
	Pure	0.2	0.4	0.6	0.8	1.0	
1.	3385	3395	3398	3395	3396	3393	Presence of H <sub>2</sub> O molecules (free water symmetric stretch)
2.	2343	2315	2302	2334	2345	2344	Hydrogen bonded O-H stretching
3.	1665	1665	1661	1661	1663	1667	OH <sub>2</sub> bending mode (asymmetric stretch)
4.	1098	1100	1096	1096	1098	1099	v <sub>3</sub> SO <sub>4</sub> (asymmetric stretch)
5.	757	756	759	757	756	755	v <sub>4</sub> SO <sub>4</sub> (bending mode)
6.	620	619	620	623	621	620	v <sub>4</sub> SO <sub>4</sub> (stretching vibration)
7.	425	426	420	422	425	425	H <sub>2</sub> O (bending mode, asymmetric stretch)

**Table 3: The FTIR band assignments for pure and thiourea added MSH crystals**

Sl.No	Wave numbers (cm <sup>-1</sup> ) for						Band assignment
	Pure	0.2	0.4	0.6	0.8	1.0	
1.	3385	3396	3381	3396	3395	3396	Presence of H <sub>2</sub> O molecules (free water symmetric stretch)
2.	2343	2362	2347	2375	2371	2284	Hydrogen bonded O-H stretching
3.	1665	1663	1660	1659	1664	1692	OH <sub>2</sub> bending mode (asymmetric stretch)
4.	1098	1098	1098	1099	1101	1098	v <sub>3</sub> SO <sub>4</sub> (asymmetric stretch)
5.	757	759	758	751	749	756	v <sub>4</sub> SO <sub>4</sub> (bending mode)
6.	620	619	617	625	624	623	v <sub>4</sub> SO <sub>4</sub> (stretching vibration)
7.	425	424	420	435	440	430	H <sub>2</sub> O (bending mode, asymmetric stretch)

# International Journal of Innovative Research in Science, Engineering and Technology

(An ISO 3297: 2007 Certified Organization)

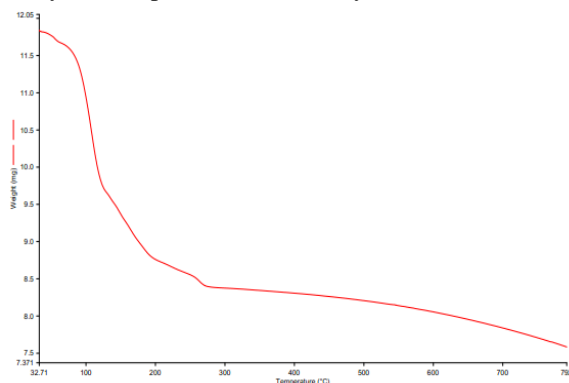
Vol. 4, Issue 7, July 2015

The sulphate anion ( $\text{SO}_4^{2-}$ ) presents four normal modes in the infrared region: a non-degenerate symmetric bending  $\nu_1$ , a doubly degenerate symmetric bending  $\nu_2$ , and two triply degenerate asymmetric stretching and bending  $\nu_3$  and  $\nu_4$  respectively [41]. Changes in solvation, metal complexation and protonation of  $\text{SO}_4^{2-}$  can modify S – O bond length and, as a result, may change the symmetry of the anion. This leads to a shift in the vibrational bands to different wave numbers and causes the degenerate vibrations to become non-degenerate.

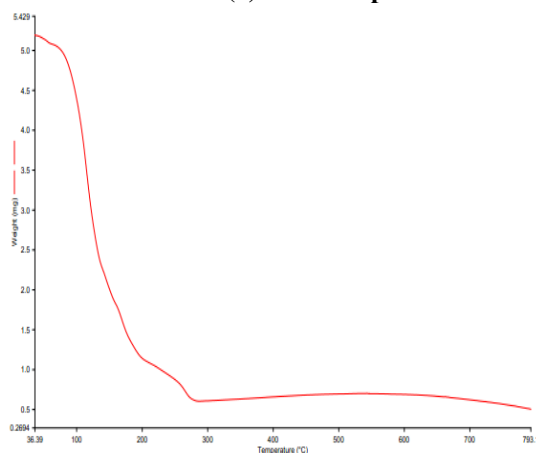
The asymmetric sulphate stretch  $\nu_3$  appears at  $1098\text{ cm}^{-1}$ . The bending modes of sulphate ( $\nu_4$ ) are positioned at around  $757$  and  $620\text{ cm}^{-1}$ . The broad envelope around  $3385\text{ cm}^{-1}$  indicates the presence of water and it belongs to free water symmetric stretch. The asymmetric stretch of water has been observed at  $1665\text{ cm}^{-1}$ . The hydrogen bond O-H stretching frequency has been observed at  $2343\text{ cm}^{-1}$ , i.e., in the region between  $2000$  and  $3200\text{ cm}^{-1}$  [41]. The corresponding water bending mode has been observed at around  $425\text{ cm}^{-1}$ . The observed spectrum for the pure MSH crystal is in correspondence with that reported in the literature [41-44].

### III.3. Thermal and optical properties

The TGA patterns observed in the present study for pure and maximum concentrated impurity added MSH crystals are shown in Figure 8. The TGA curves show that there is a rapid weight loss starting at about  $70^\circ\text{C}$  and continuing upto about  $260^\circ\text{C}$ . This weight loss may be due to the removal of water molecules. The patterns observed for the impurity added crystals are very similar to that observed for the pure MSH crystal. So, the crystals grown in the present study can be considered to be thermally stable upto about  $70^\circ\text{C}$  only.



(a) For pure

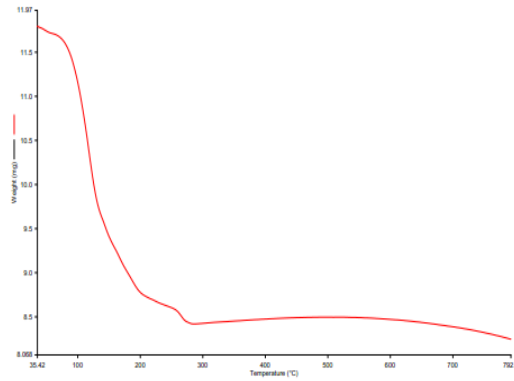


(b) For urea added

# International Journal of Innovative Research in Science, Engineering and Technology

(An ISO 3297: 2007 Certified Organization)

Vol. 4, Issue 7, July 2015



(c) For thiourea added

Figure 8: The TGA patterns observed for pure and 1.0 mole% impurity added MSH crystals

The UV-Vis-NIR transmittance spectra observed in the present study for the pure and impurity added MSH crystals are shown in Figures 9-10. All the spectra show wide transmission window in the UV-Vis-NIR region (starting from UV region with wavelength less than 250nm) which enables these crystals to be potential candidates for opto-electronic applications. As efficient nonlinear optical (NLO) crystals are expected to have optical transparency lower cut-off wavelengths between 200 and 400 nm [24], it can be understood that the crystals grown in the present study can be considered as promising NLO crystals.

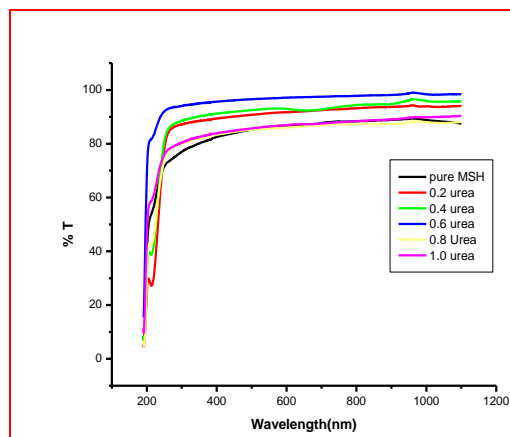
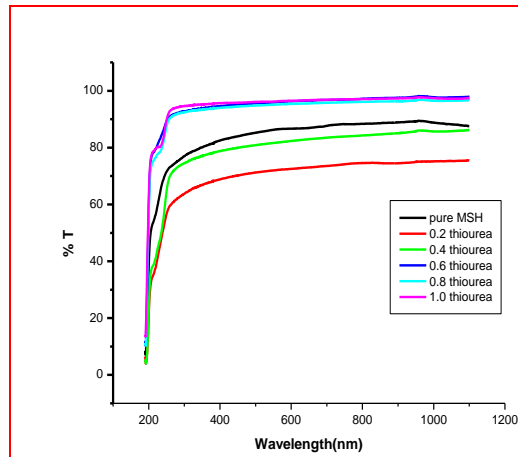


Figure9: The UV-Vis-NIR transmittance spectra of pure and urea added MSH crystals



**Figure 10: The UV-Vis-NIR transmittance spectra of pure and thiourea added MSH crystals**

The transmittance for the pure MSH crystal has been observed to be about 83% in the entire transparent region. Urea addition increases the transmittance but not systematically with the concentration. A maximum transmittance of about 95% has been observed for the 0.6 mole% urea added MSH. Also, 0.2 and 0.4 mole% urea addition leads to a transmittance of about 90%. However, the other (0.8 and 1.0 mole%) urea added MSH crystals exhibit about 83% transmittance almost like the pure MSH crystal.

In the case of thiourea added MSH crystals, the higher thiourea concentrations (0.6, 0.8 and 1.0 mole%) lead to increase in the transmittance to about 95%. The other two (0.2 and 0.4 mole%) concentrations lead to decrease in the transmittance (65 and 60% for the 0.2 and 0.4 mole% respectively). Thus, it can be stated that the higher concentrated thiourea addition and lower concentrated urea addition improve the transmittance of the MSH crystal.

#### III.4. Mechanical properties

The Vicker's hardness numbers ( $H_v$ ) observed for various loads ( $P$ ) in the present study for all the eleven crystals grown are shown in Figures 11-12. Plots of  $\log P$  versus  $\log d$  are shown in Figures 13-14. These plots are found to be nearly linear agreeing with Meyer's law.

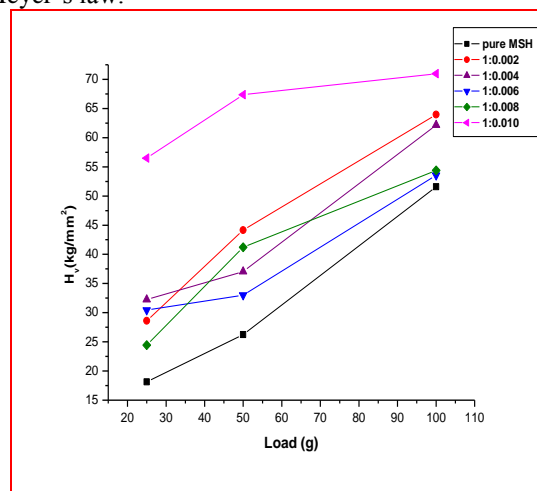


**Figure 11: Vicker's hardness number ( $H_v$ ) versus load ( $P$ ) plots for pure and urea added MSH single crystals**

# International Journal of Innovative Research in Science, Engineering and Technology

(An ISO 3297: 2007 Certified Organization)

Vol. 4, Issue 7, July 2015

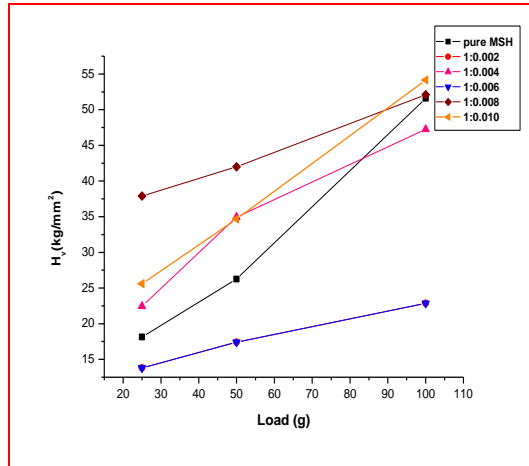


Figure 12: Vicker's hardness number ( $H_v$ ) versus load ( $P$ ) plots for pure and thioureaadded MSH single crystals

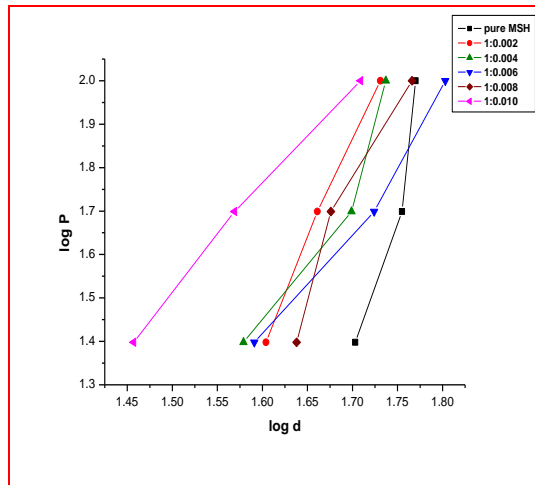
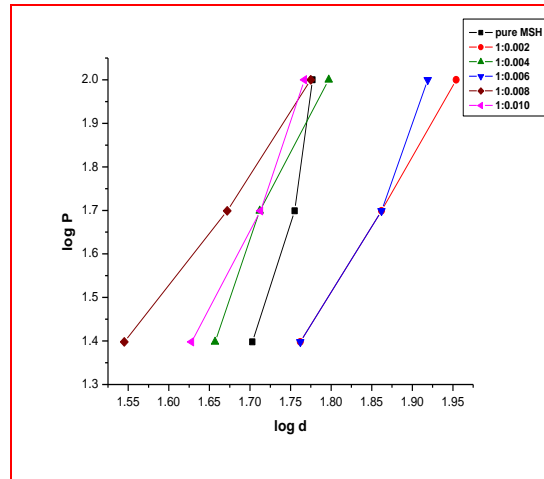


Figure 13: Plots of  $\log P$  versus  $\log d$  for pure and urea added MSH single crystals

# International Journal of Innovative Research in Science, Engineering and Technology

(An ISO 3297: 2007 Certified Organization)

Vol. 4, Issue 7, July 2015



**Figure 14: Plots of log P versus log d for pure and thiourea added MSH single crystals**

The Vicker's hardness number is found to increase with the increase in load for all the eleven crystals considered in the present study. However, there is no systematic variation observed with the impurity concentration. The work hardening coefficients (n, the Meyer index) observed are 8.197 for the pure MSH, and 15.873, 12.658, 9.434, 15.625 and 7.937 respectively for 0.2, 0.4, 0.6, 0.8 and 1.0 mole% urea added MSH, and 10.417, 14.286, 12.821, 8.696 and 14.493 respectively for 0.2, 0.4, 0.6, 0.8 and 1.0 mole% thiourea added MSH. The n values are nearly more for the impurity added MSH crystals. However, this also does not vary systematically with impurity concentration.

Combining equations (2) and (3), we have:

$$\begin{aligned}
 H_v &= (1.8544)K_1d^{n-2} \\
 \text{or } H_v &= (1.8544)K_1^{(1+2/n)} P^{(1-2/n)} \\
 \text{or } H_v &= bP^{(n-2)/n} \quad (7)
 \end{aligned}$$

where  $b = (1.8544)K_1^{(1+2/n)}$ , a new constant. The above expression shows that  $H_v$  should increase with the same if n is greater than 2. This is in good agreement with the experimental data observed in the present study and thus confirms the normal indentation size effect (ISE). Phenomenon of dependence of microhardness of a solid on the applied load at low level of testing load is known as indentation size effect [31].

According to Onitsch [45] and Hanneman [46] 'n' should lie between 1 and 1.6 for hard materials and above 1.6 for soft ones. Thus, MSH belongs to soft material category. Hence, the experimental results obtained in the present study follow the normal ISE trend.

### III.5. Electrical properties

The electrical parameters, viz.  $\sigma_{dc}$ ,  $\epsilon_r$ ,  $\tan\delta$  and  $\sigma_{ac}$  obtained in the present study are shown in Figures 15-22. The  $\sigma_{dc}$ ,  $\epsilon_r$ ,  $\tan\delta$  and  $\sigma_{ac}$  values are found to increase with the increase in temperature. This is a normal dielectric behaviour. This can be understood on the basis that the mechanism of polarization is similar to the conduction process. The electronic exchange of the number of ions in the crystal gives local displacement of electrons in the direction of the applied field, which in turn gives rise to polarization.

# International Journal of Innovative Research in Science, Engineering and Technology

(An ISO 3297: 2007 Certified Organization)

Vol. 4, Issue 7, July 2015

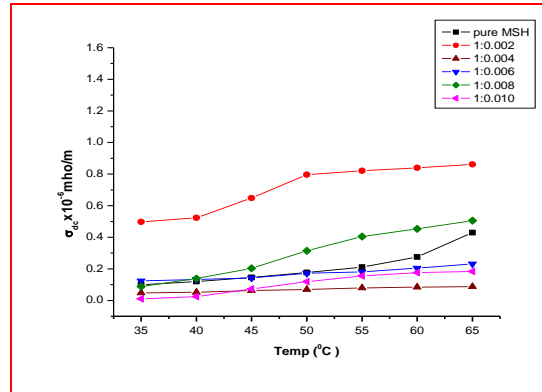


Figure 15: The DC electrical conductivities for pure and urea added MSH single crystals

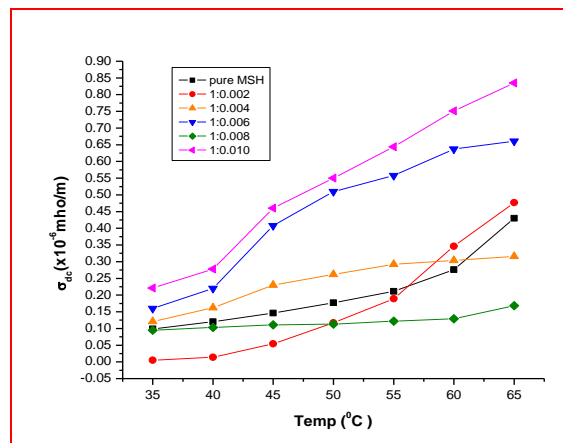


Figure 16: The DC electrical conductivities for pure and thiourea added MSH single crystals

# International Journal of Innovative Research in Science, Engineering and Technology

(An ISO 3297: 2007 Certified Organization)

Vol. 4, Issue 7, July 2015

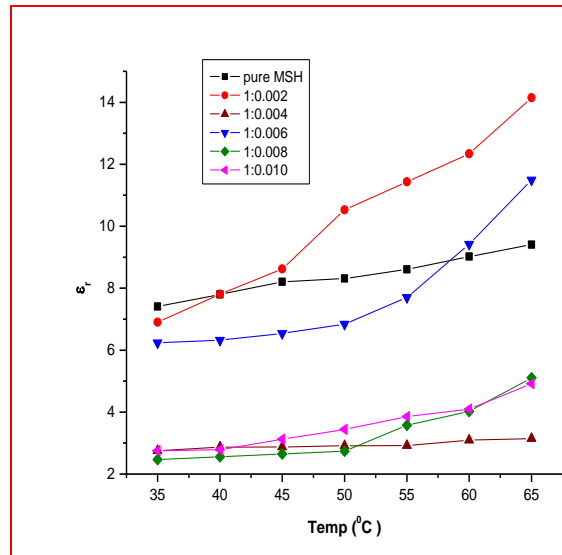


Figure 17: The dielectric constants for pure and urea added MSH single crystals

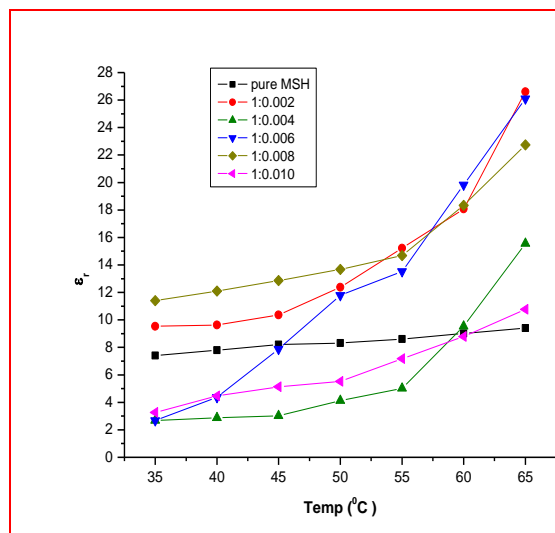


Figure18: The dielectric constants for pure and thiourea added MSH single crystals

# International Journal of Innovative Research in Science, Engineering and Technology

(An ISO 3297: 2007 Certified Organization)

Vol. 4, Issue 7, July 2015

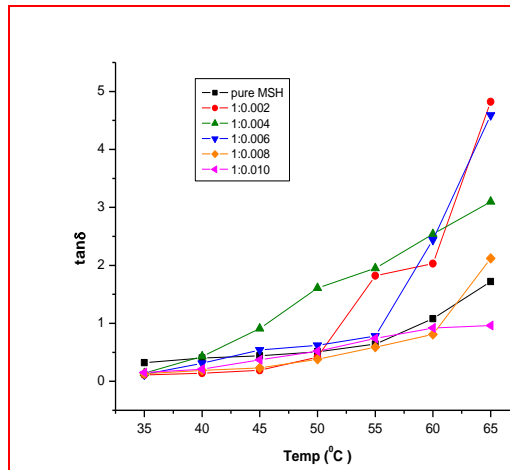


Figure 19: The dielectric loss factors for pure and urea added MSH single crystals

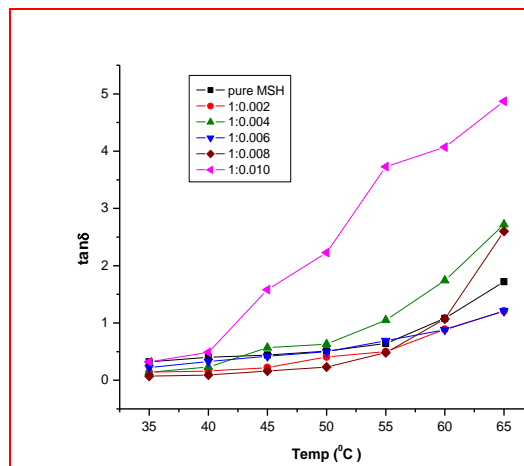


Figure 20: The dielectric loss factors for pure and thiourea added MSH single crystals

# International Journal of Innovative Research in Science, Engineering and Technology

(An ISO 3297: 2007 Certified Organization)

Vol. 4, Issue 7, July 2015

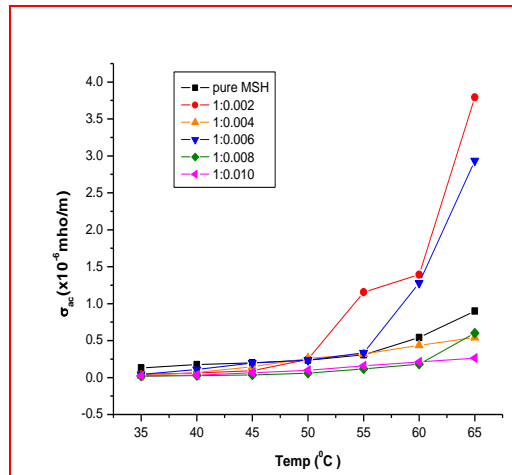


Figure 21: The AC electrical conductivities for pure and urea added MSH single crystals

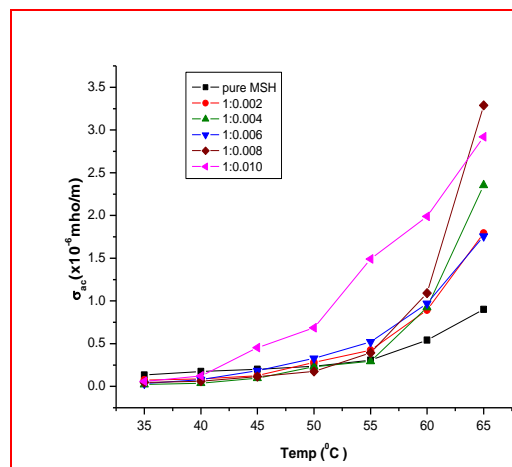


Figure 22: The AC electrical conductivities for pure and thiourea added MSH single crystals

Electrical conductivity of MSH crystals may be determined by the proton transport within the frame work of hydrogen bonds and it can be understood as due to proton movement[25]. The conduction may be due to the anions, namely  $SO_4^{2-}$  ions. The proton conduction may be accounted for by motion of protons accompanied by a D defect (excess of positive charge). Migration of these defects may only modify electric polarization and may not change the charge at an electrode [47]. The motion of defects occurs by some kind of rotation in the bond with defects. The speed of displacement  $v = va$ , where 'a' and 'v' are the distance and frequency respectively of the jump from one bond to the other. When the temperature of the crystal is increased there is a possibility of weakening of the hydrogen bonding system due to rotation of the hydroxyl ions in water molecules. The increase of conductivity with the increase in temperature observed in the present study can be understood as due to the temperature dependence of the proton transport.

Variation in  $\epsilon_r$  with temperature is generally attributed to the crystal expansion, the electronic and ionic polarizations and the presence of impurities and crystal defects. As already mentioned, the AAS data show the presence

# International Journal of Innovative Research in Science, Engineering and Technology

(An ISO 3297: 2007 Certified Organization)

Vol. 4, Issue 7, July 2015

of natural metallic impurities (Na, K, and Ca) in trace amounts. Variation of  $\epsilon_r$  at low temperatures is mainly due to the crystal expansion and electronic and ionic polarizations. Increase of  $\epsilon_r$  at higher temperatures is mainly attributed to the thermally generated charge carriers and impurity dipoles. Varotsos [48] has shown that the electronic polarizability practically remains constant in the case of ionic crystals. So, the increase in dielectric constant with temperature is essentially due to the temperature variation of ionic polarizability.

All the four electrical parameters considered in the present study, viz.  $\sigma_{dc}$ ,  $\epsilon_r$ ,  $\tan\delta$  and  $\sigma_{ac}$  do not vary systematically with the impurity concentration in the solution used for the growth of single crystals. As already mentioned, the urea and thiourea are simple organic substances and are expected to occupy the interstitial positions. Further, the density measurement shows a small decrease of density with the increase of impurity concentration taken in the solution used for the growth of single crystals. Moreover, the impurity molecules can be assumed to replace the water molecules and ions ( $Mg^{2+}$  and  $SO_4^{2-}$ ) to some extent in addition to occupying interstitials in the MSH crystal matrix creating a disturbance in the hydrogen bonding system. As the conduction in MSH is protonic and mainly due to the water molecules and  $SO_4^{2-}$  ions, the disturbance in the hydrogen bonding system may cause the conductivity to vary nonlinearly with the impurity concentration.

It is interesting to note that impurity addition (with some concentrations) leads to a reduction of dielectric constant significantly and consequently leads to low- $\epsilon_r$  value dielectric material which is gaining more importance nowadays. 0.4, 0.8 and 1.0 mole% urea addition and 0.4 mole% thiourea addition lead to reduction of  $\epsilon_r$  value significantly. The present study along with a previous study [25] made on investigating the effect of simple organic compounds as impurities on the dielectric properties of MSH crystal indicates that the oxygen content of the impurity may be a considerable factor in choosing the impurity for reducing the  $\epsilon_r$  value. So, in the present study, urea may be considered to be a better choice than thiourea in reducing the  $\epsilon_r$  value.

## IV CONCLUSIONS

Pure and urea/thiourea added  $MgSO_4 \cdot 7H_2O$  single crystals were grown by the free evaporation method at room temperature and characterized structurally, chemically, thermally, optically, mechanically and electrically. Density and lattice volume variations indicate that the impurity molecules have entered into the  $MgSO_4 \cdot 7H_2O$  crystal matrix. All the eleven crystals grown are found to be stable in the atmospheric air, non-hygroscopic, thermally stable up to about 70°C, optically transparent in the wavelength range 210-1100nm, mechanically soft and exhibit normal dielectric behaviour. AC and DC electrical measurements indicate that the electrical conduction is due to proton transport. The present study indicates that doping  $MgSO_4 \cdot 7H_2O$  with urea/thiourea leads to tuning (modifying) optical, mechanical and electrical properties of  $MgSO_4 \cdot 7H_2O$  crystal. Doping also leads to the discovery of new promising low- $\epsilon_r$  value dielectric materials.

## REFERENCES

- [1] F.M.Rayan, W.Lehmann, D.W.Feldman and J.Murphy, *J.Electrochem.Soc.-Solid State Sci.Technol.*, p.1475, 1974
- [2] M.Ikeya, G.M.Hassan, H.Sasaoka, Y.Kinoshita, S.Takaki and C.Yamanaka, *Appl.Radiat.Isotopes* **52**, 1209, 2000
- [3] R.W.G.Wyckoff, *Crystal Structures (2<sup>nd</sup> edn)* [Interscience, New York, 1960]
- [4] W.H.Baur, *Acta Crystallogr.* **17**, 1361, 1964
- [5] S.Deminkaya, O.Vural, Z.Gokail, Z.Odabashi, F.Ozdag, E.Erolu and M.Yardim, *Norol Bil D.* **15(3)**, 131, 1998
- [6] M.Ema, A.Gebrewold, B.T.Altura and B.M.Altura, *Report*, Department of Physiology, State University of New York, Health Science Centre, Brooklyn, 1998
- [7] H.Cano, N.Gabas and J.P.Canselier, *J.Cryst.Growth* **224**, 335, 2001
- [8] G.Sugaldino, G.Vaccari, D.Aquilano and M.Rubbo, *J.Cryst.Growth* **83**, 523, 1987
- [9] S.Ramalingam, J.Podder and S.N.Kalkura, *Cryst.Res.Technol.* **36**, 1357, 2001
- [10] I.A.Kasatkin, *Cryst.Res.Technol.* **37**, 193, 2002
- [11] S.Karan and S.P.Sen Gupta, *Indian J.Phys.* **80**, 781, 2006
- [12] C.K.Mahadevan, *Physica B.* **403**, 57, 2008
- [13] S.Ferdous and J.Podder, *J.Bangladesh Acad.Sci.* **33**, 47, 2009
- [14] M.Rubbo, D.Aquilano and M.F.Angela, *J.Cryst.Growth* **71**, 470, 1985
- [15] S.A.Jibbouri, C.Strege and J.Ulrich, *J.Cryst.Growth* **236**, 400, 2002
- [16] K.Jayakumari and C.Mahadevan, *J.Optics* **21**, 22, 1992
- [17] K.Jayakumari, C.Mahadevan and D.Chandrasekharam, *J.Pure&Appl.Phys.* **5**, 331, 1993

# International Journal of Innovative Research in Science, Engineering and Technology

(An ISO 3297: 2007 Certified Organization)

Vol. 4, Issue 7, July 2015

- [18] M.Theivanayagam and C.Mahadevan, *Bull.Mater.Sci.***24**, 441, 2001
- [19] K.Visscher, J.B.J.Veldhuis, H.A.J.Oonk, P.J.vanEkeren and J.G.Blok, *ECN Report ECN-C - 04-074*, 2004
- [20] V.M.van Essen, H.A.Zondag, J.Cot Gores, L.P.J.Bleijendaal, M.Bakker, R.Schuitema, W.G.J.vanHelden, Z.He and C.C.M. Rindt, *J.Solar Energy Engg.***131**, 041014, 2009
- [21] D.Hatton, K.Landskron, W.J.Hunks, M.Bennett, D.Shukaris, D.D.Perovic and G.A.Ozin, *Materials Today*, **9(3)**, 22, 2006
- [22] S.Goma, C.M.Padma and C.K.Mahadevan, *Mater.Lett.***60**, 3701, 2006
- [23] M.Meena and C.K.Mahadevan, *Cryst.Res.Technol.*, **43**, 166, 2008
- [24] J.M.Kavitha and C.K.Mahadevan, *Int.J.Eng.Res.Appl.*, **3(5)**, 1931, 2013
- [25] J.M.Kavitha and C.K.Mahadevan, *IOSR J.Appl.Phys.*,**5(4)**, 45, 2013
- [26] T.H.Freeda and C.Mahadevan, *Bull.Mater.Sci.*, **23**, 335, 2000
- [27] K.Jayakumari and C.K.Mahadevan, *J.Phys.Chem.Solids*, **66**, 1705, 2005
- [28] T.H.Freeda and C.Mahadevan, *Pramana-J.Phys.*,**57**, 829, 2001
- [29] J.A.Dean(Eds.), *Lange's Handbook of Chemistry (12<sup>th</sup>edn.)* [McGraw Hill Book Company, New York, 1979][31]
- [30] H.Lipson and H.Steeple, *Interpretation of X-ray Powder Diffraction Patterns* [MacMillan, New York, 1970]
- [31] S.Karan and S.P.Sen Gupta, *Mater.Sci.Engg.*, **A398**, 198, 2005
- [32] S.Perumal and C.K.Mahadevan, *Physica B.* **367**, 172, 2005
- [33] G.Selvarajan and C.K.Mahadevan, *J.Mater.Sci.*, **41**, 8218, 2006
- [34] N.Manonmani, C.K.Mahadevan and V.Umayorubhagan, *Mater.Manuf.Processes***22**, 388, 2007
- [35] N.Neelakanta Pillai and C.K.Mahadevan, *Mater.Manuf.Processes*,**22**, 393, 2007
- [36] N.Manonmani, C.K.Mahadevan and V.Umayorubhagan, *Mater.Manuf.Processes*,**23**, 152, 2008
- [37] C.K.Mahadevan and K.Jayakumari, *Physica B.***403**, 3990, 2008
- [38] M.Priya and C.K.Mahadevan, *Physica B.*,**403**, 67, 2008
- [39] M.Meena and C.K.Mahadevan, *Mater.Lett.*,**62**, 3742, 2008
- [40] I.Bunget and M.Popescu, *Physics of Solid Dielectrics* [Elsevier, New York, 1984]
- [41] E.Ruiz – Agudo, C.V.Putnis and C.Rodriguez – Navarro, *Crystal Growth & Des.*,**8**, 2665, 2008
- [42] S.Ramalingam, J.Podder, S.N.Kalkura and G.Bocelli, *J.Cryst.Growth*,**247**, 523, 2003
- [43] R.M.Silvenstein, G.C.Bassler and T.C.Morrill, *Spectrometric Identification of Organic Compounds* [Wiley, New York, 1981]
- [44] G.Pasupathi and P.Philominathan, *Mater.Lett.*, **62**, 4386, 2008
- [45] E.M.Onitsch, *Mikroskopia***2**, 131, 1947
- [46] M.Hanneman, *Metall.Manchu.* **23**, 135, 1941
- [47] H.Granicher, C.Jaccard, P.Scherrer and A.Steinemann, *Discuss.Farad.Soc.***23**, 50, 1957
- [48] P.Varotsos, *J.De.Phys.Lett.*,**39**, L79, 1978